THE VIBRO-ACOUSTIC BEHAVIOUR OF INFINITE HOMOGENEOUS AND COMPOSITE RODS: APPLICATION TO DISTRIBUTED OPTICAL FIBRE ACOUSTIC SENSORS

P Golacki ISVR Consulting, University of Southampton, UK
DJ Thompson Institute of Sound and Vibration Research, University of Southampton, UK

1 INTRODUCTION

There are many applications where monitoring of physical quantities such as strain, acoustic pressure, vibration or temperature over large distances would be beneficial, for example condition monitoring along railway lines[1], pipelines[2] or subsea cables[3]. An array of single point sensors is often costly and impractical due to amount of cabling required, so ideally a sensor in the form of a long cable continuously monitoring the spatial distribution of a disturbance would be a desirable solution. Optical fibres are excellent candidates due to the low cost of the fibre; moreover, the opto-electronic technology is well established due to use of optical fibres in telecommunications.

A large amount of research has been carried out on the subject of distributed optical fibre sensing[4–7] This is understandably focused on the design, analysis and improvement of the opto-electronic measurement systems. In comparison, little has been written about the vibro-acoustic response of distributed optical fibre sensors, despite the fact that theoretical analysis of structural dynamics and acoustics is very well established, and the analytical and numerical tools are available. This paper is a step to bridge this gap.

The paper is structured as follows: firstly the principles of operation of distributed optical fibre sensors are explained briefly. This is followed by a theoretical analysis of the dynamic behaviour of a homogeneous fibre. This analytical model is then compared with results from a finite element model. Some numerical results for a clad fibre are also presented.

2 DISTRIBUTED OPTICAL SENSORS - PRINCIPLE OF OPERATION

One of the first reviews on the possibility of using optical fibres for distributed sensing was by Rogers in the 1980s[8,9]. A more recent review is given by Masoudi et al.[10] Taylor and Lee[11] proposed a distributed sensor for detecting intruders in 1993.

A distributed sensor utilises light scattering in the fibre. A pulse of light is sent through the fibre and backscattered light is detected by photodetectors. When the optical fibre is disturbed this causes a phase change of the scattered light wave. The basic relationship describing the phase ϕ of a light wave propagating through the fibre is[12,13]:

$$\phi = \beta L \tag{1}$$

where β is the propagation constant (wavenumber), given by

$$\beta = \frac{2\pi n}{\lambda} \tag{2}$$

where n is the effective refractive index of the optical fibre and λ is wavelength of the light source. L is the distance travelled by the light wave. The change in the phase of a light wave due to a mechanical disturbance is:

$$\Delta\phi = \beta\Delta L + L\Delta\beta \tag{3}$$

The first term is due to physical length changes of the section of fibre and the second is due to changes in propagation constant, which contains two terms:

$$L\Delta\beta = L\frac{\mathrm{d}\beta}{\mathrm{d}n}\Delta n + L\frac{\mathrm{d}\beta}{\mathrm{d}D}\Delta D \tag{4}$$

The first of these terms is due to the change of refractive index n and the second is due to changes in diameter (waveguide mode dispersion effect). The effect of changes in diameter is negligible as it is three orders of magnitude lower than the changes of length and refractive index.[13]

When an external pressure ΔP is applied to the fibre, the phase sensitivity per unit pressure and length is given by (see Refs. [12–14] for details):

$$\frac{\Delta\phi}{\Delta PL} = \beta\left\{\epsilon_z - \frac{1}{2}n^2[(p_{11}+p_{12})\epsilon_r + p_{12}\epsilon_z]\right\} \tag{5}$$

where p_{11}, p_{12} are photo-elastic constants and ϵ_r, ϵ_z are strains in the radial and axial directions. Since β is dependent on the wavelength of the light source, the source independent "normalised" phase sensitivity is introduced:

$$\frac{\Delta\phi}{\Delta P\beta L} = \epsilon_z - \frac{1}{2}n^2[(p_{11}+p_{12})\epsilon_r + p_{12}\epsilon_z] \tag{6}$$

This simple relationship shows that the phase of the light is dependent mainly on the axial and radial strains and the photo-elastic parameters of the optical fibre.

Three scattering mechanisms exists in the optical fibres, namely Rayleigh scattering, Brillouin scattering and Raman scattering. However, only the Brillouin and Rayleigh scattering processes are sensitive to strain in the fibre[4]. Rayleigh scattering occurs due to density fluctuations in the fibre. These inhomogeneities are created during manufacturing process of the fibre. Brillouin scattering, on the other hand, is the effect of the interaction between the light and acoustic phonons, which are thermally generated acoustic waves[4].

Practical implementation of a distributed optical fibre sensor system requires an optical fibre interrogation technique. Various techniques exist for both scattering processes. For Rayleigh scattering Phase Optical Time Domain Reflectometry (φ-OTDR) is the most promising. Frequency domain methods also exist but have a more limited strain range. Techniques for the Brillouin process include Brillouin optical time domain reflectometry, Brillouin optical time domain analysis and Brillouin optical correlation-domain analysis[4].

Brillouin scattering sensors have several disadvantages such as limited frequency range, short sensing range, long averaging time needed to extract the desired signal, and low strain resolution. Rayleigh scattering sensors can achieve a higher signal-to-noise ratio, a broader frequency range and a longer spatial range[3]. One of the main features of the Rayleigh scattering sensors is that only the relative phase of the backscattered light between the ends of the gauge section is measured, which can affect the accuracy of the measurement, as only the net elongation across the gauge will be measured[3,4].

3 VIBRO-ACOUSTIC RESPONSE OF A HOMOGENEOUS ROD

Dynamically, an optical fibre can be modelled as a cylindrical rod. The core is usually made of silica glass; and additional layers of material can be added to protect the fibre from the environment, which can affect the amplitude of vibration in the fibre. Different coatings could be used to enhance or reduce the sensitivity to external pressure or stress[12,15]. For simplicity the analysis begins with a homogeneous rod before considering the effect of the cladding on the acoustic response of the fibre.

In the current study a number of simplifying assumptions are made. The rod diameter is assumed to be much smaller than the wavelength of the acoustic excitation. The diameter of standard optical

fibres is 0.4 mm, although this may vary depending on the actual type of fibre. This does not include any potential additional cladding. The pressure gradient around the fibre is assumed to be negligible, so the pressure excitation is taken as axisymmetric. The material damping is neglected in the current model. Acoustic excitation is simplified to be either a section of uniform pressure or a section of pressure which varies spatially as a cosine function to simulate a spatially windowed plane wave excitation. The fibre is treated as a rod and no additional tensile stress is included.

Since axisymmetric excitation is assumed, one can expect that only longitudinal waves will be generated in the fibre. This suggests taking a similar approach as in the well-known derivation of the equation of motion for longitudinal vibration of a rod[16,17]:

$$\frac{\partial^2 u_z}{\partial z^2} - \frac{1}{c^2}\frac{\partial^2 u_z}{\partial t^2} = F_z e^{\mathrm{j}\omega t} \tag{7}$$

where u_z is the axial displacement, z is spatial coordinate along the axis of the rod, t is time and c is the wavespeed of longitudinal waves in the rod, given by:

$$c = \sqrt{\frac{E}{\rho}} \tag{8}$$

with *E* the Young's modulus and ρ the density. In the above equation an external axial harmonic force (per unit length) $F_z e^{\mathrm{j}\omega t}$ at circular frequency ω acts along the axis of the rod. In the case of an optical fibre sensor, the excitation acts radially on the outer surface of the fibre and the longitudinal waves are generated due to the Poisson's effect. One needs to determine the equivalent axial force due to this radial excitation. This is done by using the full stress-strain relationship:

$$\sigma_z = E\epsilon_z + \nu(\sigma_r + \sigma_\varphi) \tag{9}$$

where σ_k is the stress component and subscripts $k = r, \varphi, z$ denote radial, angular and axial components respectively, ϵ_z is the axial strain. Note that usually in the derivation of the equation of motion for rods only the simplified stress-strain relationship is used:

$$\sigma_z = E\epsilon_z \tag{10}$$

From the theory of elasticity it is known that for an axisymmetric stress distribution the radial stress of a circular cross-section is equal to the angular stress[18]:

$$\sigma_r = \sigma_\varphi \tag{11}$$

When equation (9) is used in the usual derivation of the equation of motion for longitudinal waves in the rod instead of equation (10), the modified equation of motion will be:

$$\frac{\partial^2 u_z}{\partial z^2} - \frac{1}{c^2}\frac{\partial^2 u_z}{\partial t^2} = -\frac{2\nu}{E}\frac{\partial \sigma_r}{\partial z} \tag{12}$$

Equation (12) shows that the amplitude of the vibration in the rod excited radially will be proportional to the Poisson's ratio of the material and inversely proportional to the Young's modulus.

To determine the response of the fibre, the radial stress is equated to the external pressure. Consider a simple excitation consisting of a uniform, axisymmetric harmonic pressure acting over a length L. It can be defined as:

$$\sigma_r(z,t) = -P(z) = -Pe^{\mathrm{j}\omega t}\Pi\left(\frac{z}{L}\right) \tag{13}$$

where $\Pi\left(\frac{z}{L}\right)$ is the rectangular function over the section L. The derivative of the rectangular function is given by the sum of two Dirac deltas:

$$\frac{\partial\left(\Pi\left(\frac{z}{L}\right)\right)}{\partial z} = \delta\left(z + \frac{L}{2}\right) - \delta\left(z - \frac{L}{2}\right) \tag{14}$$

So the equation of motion with the external forcing can be written as:

$$\left(\frac{\partial^2 u_z}{\partial z^2} - \frac{1}{c^2}\frac{\partial^2 u_z}{\partial t^2}\right) = \frac{2\nu P}{E}\left[\delta\left(z + \frac{L}{2}\right) - \delta\left(z - \frac{L}{2}\right)\right] e^{\mathrm{j}\omega t} \tag{15}$$

The solution to the equation of motion for excitation by a Dirac delta is well-known; it was derived for strings and is available in number of acoustics textbooks such as Morse and Ingard[19]. For excitation by $\delta(z - z_0)$ the solution is[17]:

$$G(z|z_0) = \frac{\mathrm{j}}{2k} e^{-\mathrm{j}k|z - z_0|} \tag{16}$$

where $k = \frac{\omega}{c}$ is the structural wavenumber. So using equation (16) in equation (15), the following expression is obtained for the axial displacement:

$$u_z(z,t) = \frac{\nu P \mathrm{j}}{Ek}\left(e^{-\mathrm{j}k\left|z + \frac{L}{2}\right|} - e^{-\mathrm{j}k\left|z - \frac{L}{2}\right|}\right) e^{\mathrm{j}\omega t} \tag{17}$$

The axial strain is obtained by differentiating the above equation:

$$\epsilon_z(z,t) = \frac{\partial u_z}{\partial z} \tag{18}$$

$$\epsilon_z(z,t) = \begin{cases} B\left(e^{-\mathrm{j}k\left|z + \frac{L}{2}\right|}\mathrm{sgn}\left(z + \frac{L}{2}\right) - e^{-\mathrm{j}k\left|z - \frac{L}{2}\right|}\mathrm{sgn}\left(z - \frac{L}{2}\right)\right) e^{\mathrm{j}\omega t}, & z \neq -\frac{L}{2} \wedge z \neq \frac{L}{2} \\ B\left(1 + e^{-|2\mathrm{j}kz|}\right) e^{\mathrm{j}\omega t}, & z = -\frac{L}{2} \vee z = \frac{L}{2} \end{cases} \tag{19}$$

When this is analysed in detail it is apparent that the motion of the fibre outside the excited region consists of outward travelling waves and that inside the excited region is a standing wave pattern dependent on the length L of the excited segment.

To determine the full response to a mechanical disturbance on the optical fibre, the radial motion is also required. Since the fibre is thin and lateral inertia can be neglected, the stress-strain relationship will suffice to calculate the radial displacement and strain. The relationship is given in equation (9). Keeping in mind that angular and radial stress are equal for the axisymmetric case and transforming stress-strain relationship (9), the radial strain is given by:

$$\epsilon_r = \frac{\sigma_r(1 - \nu - 2\nu^2)}{E} - \nu\epsilon_z \tag{20}$$

The radial displacement can be calculated by integrating the radial strain over the radial coordinate:

$$u_r(r,z,t) = \int \epsilon_r(z,t)dr = r\epsilon_r(z,t) + C \tag{21}$$

The integration constant C can be set to 0 since, for axisymmetric excitation, $u_r(0,z,t) = 0$.

4 APPROACH TO STUDY A MULTI-LAYERED ROD

According to McNiven et al.[20] and others[21–27] the exact solution for both a homogeneous and a multi-layered cylindrical rod can be derived from 3-D elasticity equations using the method of potentials and the Helmholtz decomposition in cylindrical coordinates. The resulting solution is a complicated equation involving a combination of Bessel functions of the first and second kinds. The boundary conditions required to calculate the dispersion relation (wavespeed vs. frequency) in an infinite freely vibrating clad fibre for axisymmetric motion are as follows (see McNiven et al.[20]):

i. Continuity of radial displacement at the interface between two layers $u_{r1}(R_1,z) = u_{r2}(R_1,z)$

ii. Continuity of axial displacement at the interface between two layers $u_{z1}(R_1, z) = u_{z2}(R_1, z)$
iii. Continuity of radial stress at the interface between two layers $\sigma_{r_1}(R_1, z) = \sigma_{r_2}(R_1, z)$
iv. Continuity of shear stress at the interface between two layers $\tau_{rz1}(R_1, z) = \tau_{rz2}(R_1, z)$
v. Continuity of radial stress at the outer layer of the rod $\sigma_{r2}(R_2, z) = 0$ for the dispersion calculation and $\sigma_{r2}(R_2, z) = -P(z)e^{j\omega t}$ for the acoustic excitation
vi. Shear stress vanishes at the outer layer of the rod $\tau_{rz2}(R_2, z) = 0$

Stress-strain relationships are required to connect the boundary conditions i-vi and the displacement solutions derived from the potential method. The resulting set of homogeneous equations for the "free vibration" have solutions only when determinant of the coefficients of a 6x6 matrix D is equal to zero. From setting the determinant equal to zero the dispersion relation can be calculated. The homogeneous rod excited by an external pressure only required one boundary condition, which is the continuity of stress at the outer layer of the cylinder.

The exact solution is complicated and difficult to interpret, thus the current research effort is directed towards deriving a simplified model using a one dimensional equation for the clad rod as derived by Lai[25,26] and using a plane strain approximation for the cross-section of the coated fibre[12,28,29].

5 RESULTS OF NUMERICAL AND ANALYTICAL MODELS

Finite element models have been created and used for comparison with the analytical model. Perfectly matched layers (PML) are used to simulate an infinite rod. Material parameters used in the numerical modelling are summarised in Table 1. All the parameters were taken directly from Comsol material library. The results in this section serve two purposes: to validate the analytical model and to understand the vibro-acoustic behaviour of the sensor.

Figure 1 depicts the spatial response of complex axial displacement due to a unit acoustic pressure at 10 kHz applied over a region of length $L = 0.1$ m. The analytical response was calculated using the analytical expressions from Section 3. The real part of the response can be thought of as a snapshot at $= 0$. As can be seen from Figure 1, the agreement for axial displacement is excellent apart from the perfectly matched layer (PML) regions, where the wave decays as expected.

The corresponding results for the radial strain are shown in Figure 2. Agreement between analytical and numerical models is again excellent. Moreover it can be observed that the sign of the radial strain is opposite to the axial strain which means that the second term in equation (6) partially "cancels out", which means that the sensitivity of the fibre optic sensor is in this case mainly dictated by the axial strain.

Next the FE model is used to study coated fibres. Figure 3(left) shows the axial strain response of a coated fibre for three frequencies, 100, 1000 and 10000 Hz. The coating is a generic acrylic plastic with external radius 1.25 mm, i.e. 5 times that of the fibre. The sensitivity within the excited region is largely independent of frequency, but wave effects are apparent outside the excited region at high frequencies. Figure 3(right) compares the results for the bare fibre, the coated fibre, and fibre coated with a steel casing. The acrylic coating increases the sensitivity by 26 dB (factor of 20) whereas the steel coating reduces it slightly.

Figure 4(left) shows the effect on the fibre response of increasing the outer radius of the cladding. Increasing the radius improves the sensitivity of the sensor. However there is a limit to this approach and further increasing the radius has only a small effect. Figure 4(right) shows the effect of varying the Young's modulus of the fibre coating. The results are given for different values of the ratio of Young's moduli of the coating $E1$ and the cladding $E2$, i.e. $E = E1/E2$. Decreasing the Young's modulus of the coating (i.e. larger values of E) increases the sensitivity of the response, whereas higher values make the fibre less responsive. Again there is a limit to this approach.

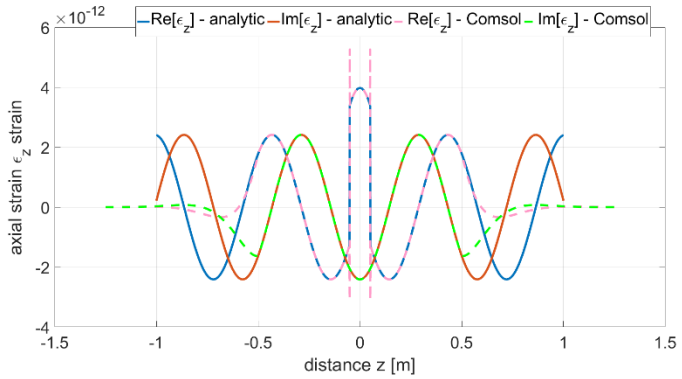

Figure 1 Comparison of complex axial strain spatial response calculated using analytical model and numerical FE model, PML located at z = ±0.5 m and PML length 0.75 m at each end. Load was applied at $-L/2 > z > L/2$, with $L = 0.1$ m. Frequency of the excitation 10 kHz. Results evaluated for homogeneous silica rod with 0.25 mm radius

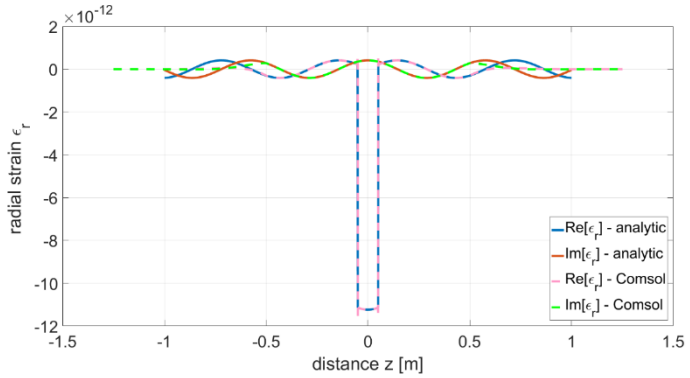

Figure 2 Comparison of complex radial strain spatial response calculated using analytical model and numerical FE model, PML located at z = ±0.5 m and PML length 0.75 m at each end. Load was applied at $-L/2 > z > L/2$, $L = 0.1$ m. Frequency of excitation 10 kHz. Results evaluated for homogeneous silica rod with 0.25 mm radius

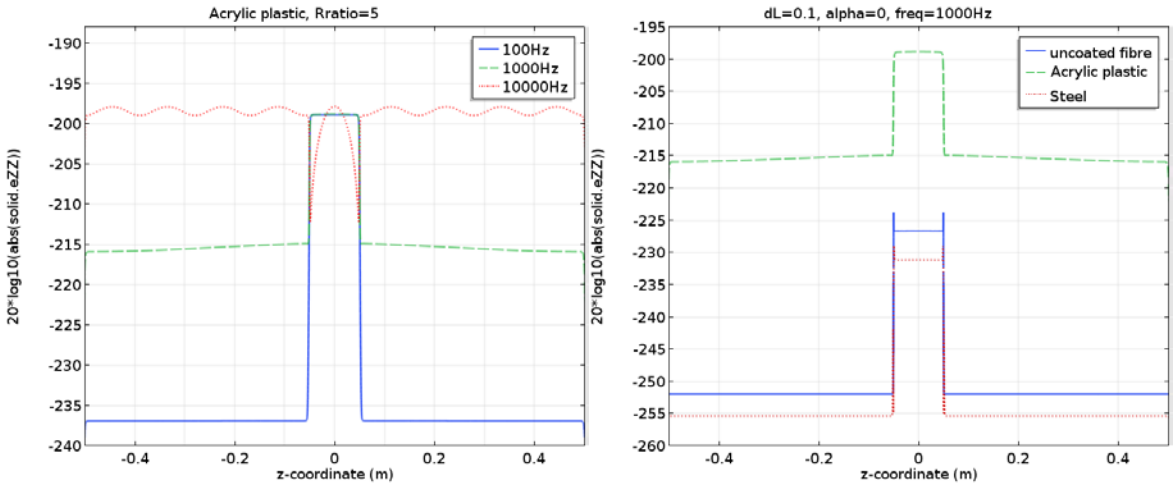

Figure 3 Magnitude of axial strain in dB ref 1. Left: fibre coated with acrylic plastic 1.25 mm radius at different frequencies. Right: comparison of bare fibre (0.25 mm radius) with different coated fibres (1.25 mm radius) at 1 kHz. Numerical FE modelling results

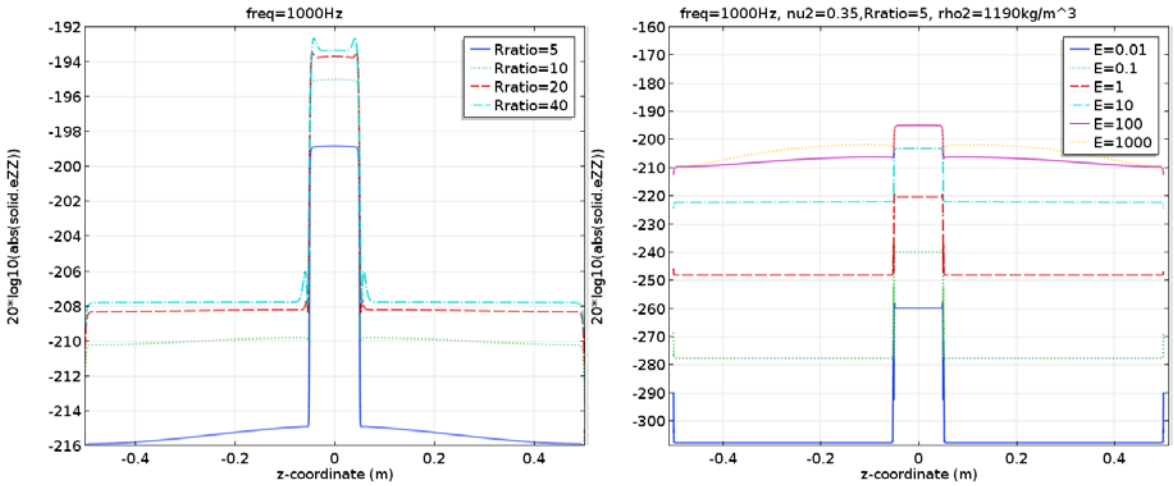

Figure 4 Effect of increasing the radius of the cladding Rratio=R2/R1 (left) and changing the Young's modulus of the coating E=E1/E2 (right) on the magnitude of the axial strain, frequency 1 kHz, L=0.1 m, Values in dB ref 1

Table 1 Summary of the material parameters ($c = \sqrt{E/\rho}$)

Material	Density ρ [kg/m^3]	Young's Modulus E[GPa]	Poisson's Ratio ν	Wave speed c[m/s]
Silica glass	2203	73.1	0.17	5760
Acrylic plastic	1190	3.2	0.35	1640
Steel	7850	205.0	0.28	5110

6 DISCUSSION AND CONCLUSIONS

An initial study has been presented of the vibrational response of a fibre excited axisymmetrically along a finite section. This is a fairly complicated phenomenon: travelling waves are generated at the edges of the excited region, which can potentially complicate interpretation of the results from the optical fibre system. It has also been shown that using a softer material for the cladding can improve the sensitivity of the sensor, in the case of a generic acrylic plastic by a factor of 20. Moreover, increasing the radius of the coating and softening of the material (reducing Young's modulus) can improve the sensitivity further; however there is a "saturation limit" for both approaches.

This study has several limitations such as neglecting damping in the fibre, so the actual extent of the travelling wave is unknown. The analytical model for the coated fibre is still under development. This model is desirable as it would help understanding of the wave generation in the fibre, it would serve as a design aid to choose an appropriate coating and also improve speed of calculation. Other important factors to consider are the photo-elastic coupling, spatial integration of the sensors along the gauge length, and the effect of relative phase detection in Rayleigh scattering based systems.

Acknowledgement

This work is funded by UK EPSRC grant (EP/N00437X/1)

7 REFERENCES

1. Minardo A, Cocetta A, Porcaro G, Giannetta D, Bernini R, Zeni L. Railway Traffic Monitoring by Use of Distributed Optical Fiber Sensors. *Proc Fourteenth Int Conf Civil, Struct Environ Eng Comput*. 2013;102(November 2014). doi:10.4203/ccp.102.28.
2. Hussels M-T, Chruscicki S, Habib A, Krebber K. Distributed acoustic fibre optic sensors for condition monitoring of pipelines. *Sixth Eur Work Opt Fibre Sensors*. 2016;9916(May

2016):99162Y. doi:10.1117/12.2236809.
3. Masoudi A, Pilgrim JA, Newson TP, Brambilla G. Subsea Cable Condition Monitoring with Distributed Optical Fibre Vibration Sensor. *J Light Technol*. 2019;(July):1-1. doi:10.1109/jlt.2019.2893038.
4. Masoudi A, Newson TP. Contributed Review: Distributed optical fibre dynamic strain sensing. *Rev Sci Instrum*. 2016;87(1). doi:10.1063/1.4939482.
5. Muanenda Y. Recent Advances in Distributed Acoustic Sensing Based on Phase-Sensitive Optical Time Domain Reflectometry. *J Sensors*. 2018;2018:1-16. doi:10.1155/2018/3897873.
6. Bao X, Chen L. Recent Progress in Distributed Fiber Optic Sensors. *Sensors*. 2012;12(12):8601-8639. doi:10.3390/s120708601.
7. Ding Z, Wang C, Liu K, et al. Distributed optical fiber sensors based on optical frequency domain reflectometry: A review. *Sensors (Switzerland)*. 2018;18(4):1-31. doi:10.3390/s18041072.
8. Rogers A. Distributed optical-fibre sensors. *J Phys D Appl Phys*. 1986;19(12).
9. Rogers AJ. Distributed optical-fibre sensors for the measurement of pressure, strain and temperature. *Phys Rep*. 1988;169(2):99-143. doi:10.1016/0370-1573(88)90110-X.
10. Masoudi A, Newson TP. High Frequency Distributed Optical Fibre Dynamic Strain Sensing : A Review. In: *EAGE/DGG Workshop on Fibre Optic Technology in Geophysics*. ; 2017. http://eprints.soton.ac.uk/403685/.
11. Taylor H. F, Lee CE. Apparatus and method for fiber optic instrusion sensing, US Patent US5194847A. 1993.
12. Hocker GB. Fiber optic acoustic sensors with composite structure: an analysis. *Appl Opt*. 1979;18(21):3679-3683.
13. Hocker GB. Fiber-optic sensing of pressure and temperature. *Appl Opt*. 1979;18(9):1445-1448. doi:10.1364/AO.18.001445.
14. Giallorenzi TG, Bucaro JA, Dandridge A, et al. Optical Fiber Sensor Technology. *IEEE Trans Microw Theory Tech*. 1982;30(4):472-511. doi:10.1109/TMTT.1982.1131089.
15. Lagakos N, Bush IJ, Cole JH, Bucaro JA, Skogen JD, Hocker GB. Acoustic desensitization of single-mode fibers utilizing nickel coatings. *Opt Lett*. 1982;7(9):460. doi:10.1364/OL.7.000460.
16. Seto WW. *Schaum's Outline of Theory and Problems of Mechanical Vibrations*. Schaum Publishing Co.; 1964.
17. Golacki P. Interim progression review report Advanced applications of distributed optical fibre sensors in acoustics. 2017;(November).
18. Timoshenko S, Goodier JN. *Theory of Elasticity*.; 1951. doi:10.1007/BF00046464.
19. Morse PM, Ingard KU. *Theoretical Acoustics*. Princeton university press; 1968.
20. McNiven HD, Sackman JL, Shah AH. Dispersion of Axially Symmetric Waves in Composite, Elastic Rods. *J Acoust Soc Am*. 1963;35(10):1602-1609. doi:10.1121/1.1918766.
21. Armenàkas AE. Propagation of Harmonic Waves in Composite Circular-Cylindrical Rods. *J Acoust Soc Am*. 1970;47(3B):822-837. doi:10.1121/1.1911965.
22. Gazis DC. Three-Dimensional Investigation of the Propagation of Waves in Hollow Circular Cylinders. I. Analytical Foundation. *J Acoust Soc Am*. 1959;31(5):568-573. doi:10.1121/1.1907753.
23. Meeker TR, Meitzler AH. Guided wave propagation in elongated cylinders and plates. In: *Physical Acoustics*. Vol 1 Part A. ; 1964:111-167.
24. Sternberg E. On the integration of the equations of motion in the classical theory of elasticity. *Arch Ration Mech Anal*. 1960;6(1):34-50. doi:10.1007/BF00276152.
25. Lai J. The propagation of waves in composite elastic rods and viscoelastic rods. 1968.
26. Lai J, Dowell EH, Tauchert TR. Propagation of Harmonic Waves in a Composite Elastic Cylinder. *J Acoust Soc Am*. 1971;49(1B):220-228. doi:10.1121/1.1912320.
27. Honarvar F, Sinclair AN. Scattering of an obliquely incident plane wave from a circular clad rod. *J Acoust Soc Am*. 1997;102(1):41-48. doi:10.1121/1.419764.
28. Budiansky B, Drucker DC, Kino GS, Rice JR. Pressure sensitivity of a clad optical fiber. *Appl Opt*. 1979;18(24):4085-4088. doi:10.1364/AO.18.004085.
29. Timoshenko SP, Goodier JN. Theory of elasticity. *McGraw-Hill B Co, Inc, New York*. 1970.